TELEMÁTICA
REVISTA DIGITAL de las Tecnologías de la Información y las Telecomunicaciones
Revista Telemática. Vol. 4 No. 20 , Octubre-Diciembre, 2021, p.40- 51 ISSN 1729-3804

SUPERVISED CLASSIFICATION OF RADAR TARGETS USING THE MOMENTS SPACE

Yusleidy Alvarez Germade[1], Camilo Guillén Soriano[2], Liz Martínez Marrero[3], Nelson Chávez Ferry[4]

[1]Technological University of Havana "José Antonio Echeverría", CUJAE, 114 Street, #11901, La Habana, Cuba
yagermade@tele.cujae.edu.cu
[2]Technological University of Havana "José Antonio Echeverría", CUJAE, 114 Street, #11901, La Habana, Cuba
camilo.gs@tele.cujae.edu.cu
[3]University of Luxembourg, 29 Avenue J.F. Kennedy, L-1855, Luxembourg, Luxembourg
liz.martinez-marrero@uni.lu
[4]Technological University of Havana "José Antonio Echeverría", CUJAE, 114 Street, #11901, La Habana, Cuba
nelson@tele.cujae.edu.cu

ABSTRACT

The computation of statistical moments of the radar echo-signals with the objective of translating the decision to the moments space has shown potential in recent work. However, the moments space has not been considered for multiple targets classification, nor its combination with supervised classifiers has been studied. This paper proposes the use of moments as input features for several supervised classifiers and evaluates their performance. Among the considered methods are the Bayesian classifier, k-nearest neighbors, Support Vector Machines and artificial neural networks. The results show the usefulness of the moments space for classifying radar targets with high accuracy, precision and low complexity.

INDEX TERMS: Radar, automatic target recognition, supervised classification, moments space.

CLASIFICACIÓN SUPERVISADA DE BLANCOS DE RADAR UTILIZANDO EL ESPACIO DE LOS MOMENTOS

RESUMEN

El cálculo de los momentos estadísticos de las eco-señales de radar con el objetivo de trasladar la decisión al espacio de los momentos ha mostrado potencialidades en trabajos recientes. No obstante, el espacio de los momentos no ha sido considerado para la clasificación de múltiples clases, ni se ha estudiado su combinación con clasificadores supervisados. Este artículo propone el empleo de los momentos como rasgos de entrada para varios clasificadores supervisados y evaluar su desempeño. Entre los métodos estudiados se encuentran el clasificador Bayesiano, k-vecinos más cercanos, Support Vector Machines y redes neuronales artificiales. Los resultados manifiestan la utilidad del espacio de los momentos para clasificar blancos de radar con elevada exactitud, precisión y baja complejidad.

PALABRAS CLAVES: Radar, reconocimiento automático, clasificación supervisada, espacio de los momentos.

1. INTRODUCTION

Automatic target recognition (ATR) in the radar field is of great importance for many applications. Among these is the growth of the fishing industry [1], environmental protection [2, 3], the fight against drugs traffic [4], as well as the rescue from natural disasters or maritime accidents [5, 6]. Of particular interest is recognizing low-velocity and small radar cross-section (RCS) objects, commonly referred to as low-observable targets [7-10].

ATR systems analyze the electromagnetic radiation from a range profile, in order to classify the process taking place in each resolution cell according to its scattering properties. For this purpose, discriminative features are extracted from the received signal to make a decision about the target's identity [11]. Among the most widely used feature

Manuscript Received: 11-02-2022 Accepted: 24-04-2022

TELEMÁTICA
REVISTA DIGITAL de las Tecnologías de la Información y las Telecomunicaciones
Revista Telemática. Vol. 4 No. 20 , Octubre-Diciembre, 2021, p.40- 51 ISSN 1729-3804

extraction techniques in the radar field are subspace methods [12] and principal component analysis (PCA) [8, 13], which are combined with supervised classifiers such as Support Vector Machine (SVM) [12, 14], Artificial Neural Networks (ANN) [1, 5, 12] and k-nearest neighbors [4, 15].

In this scenario, it is convenient to find features that improve the overall performance of the classifier, with low computational complexity and free from the statistical distribution of the echo-signals. Recently, progress has been made in a technique that offers advantages in all three of the above aspects and is called detection in the moments space [16, 17]. Its essence lies in transferring the decision-making to the space formed by a certain number of statistical moments (mean, average power, etc.) computed from the echo-signal parameters (amplitude, frequency, etc.) [17].

The theoretical framework of this technique, presented in previous works [16-18] from a detection point of view (binary classification), is based on the assignment of each resolution cell to the background or anomaly classes. Then, it is identified as a problem that the moments space has not been considered for the classification of multiple classes, nor its combination with supervised classifiers. Therefore, the objectives of this paper are to propose the moments as input features for several supervised classifiers [11] and to evaluate their performance. The results obtained show the usefulness of the moments space for the classification of radar targets with high accuracy, precision and low complexity.

The following section defines the basics for classification in the moments space. The third section presents some of the most widespread supervised classifiers, while the four evaluates their performance for five types of targets and discuss the obtained results.

2. THE MOMENTS SPACE FOR RADAR CLASSIFICATION

In the following, the only considered parameter will be the amplitude of the video signal for a monostatic pulse radar that scans a two-dimensional superficial searching window (range and azimuth) [19]. The index $u = 1, \ldots, U$ identifies the U resolution cells that compose the window, whose dimensions will depend on the range and azimuth resolutions.

The amplitude of the video signal is a continuous random process. By properly sampling this process [16, 19], it is possible to associate to each resolution cell a set of samples Ψ_u, which will be a discrete random process often referred to as cellular emission. If any anomaly occurs in the searching window, the corresponding cellular emission Ψ_u will carry out information about the produced changes. As the "natural" behavior of Ψ_u is affected, the variation will be reflected in the moments that determine its joint probability density of statistic order G [20]. By selecting S moments and sorting them according to the indices 1, 2, … S, it is possible to compute N values for each one and associate to each resolution cell the set

$$\Phi_u = \{\boldsymbol{\mu}\}_{n=1,\ldots,N} = \{\varepsilon_1, \varepsilon_2, \ldots, \varepsilon_S\}_{n=1,\ldots,N} \tag{1}$$

formed by N vectors (or patterns) denoted by $\boldsymbol{\mu}$, whose components (or features) $\varepsilon_1, \varepsilon_2, \ldots, \varepsilon_S$ are the moments. Thus, the statistical behavior of any cellular emission is characterized by Φ_u in an S-dimensional space: the moments space.

The expression for computing N values of the s-th moment from N random samples of size M is given by

$$\{\varepsilon_s\}_{n=1,\ldots,N} = \frac{1}{M}\sum_{m=1}^{M} \mathrm{X}_{m,n} = \frac{1}{M}\sum_{m=1}^{M}\left[\prod_{g=1}^{G} x_g^{l_g}\right]_{m,n} \tag{2}$$

where $\mathrm{X} = \prod_{g=1}^{G} x_g^{l_g}$ is a sample element composed by the samples of the video signal $x_1, \ldots, x_G$ multiplied and raised to the corresponding l_g. The sum $L = \sum_{g=1}^{G} l_g$ is the moment order for the statistic order G [20, 21].

The goal of the supervised classification through the moments space is to use the information contained in Φ_u to assign each resolution cell to one of the considered classes. Note that the computation of moments only involves accumulation and multiplication operations, which does not require high consumption of hardware or software resources. Hence the low complexity associated with the use of moments as input features for classification.

3. SUPERVISED CLASSIFICATION METHODS USING THE MOMENTS SPACE

A supervised classifier using the moments space receives at the input a pattern **μ** and its goal is to assign it to one of the *C* classes studied and labeled beforehand. Among the supervised classifiers used in the radar field are the Bayesian classifier [22, 23], k-nearest neighbors (knn) [4, 15], Support Vector Machine (SVM) [12, 14] and Artificial Neural Networks (ANN) [1, 5, 12]. We define next each method and specify its use when the input features are the moments.

Bayesian classifier

Given a pattern $\boldsymbol{\mu} \in \mathbb{R}^S$ (with $\mathbb{R}^S$ denoting the S–dimensional Euclidean space) defined in the previous section and a set of *C* classes $\{c_i\}$, $i = 1, 2, \ldots, C$, a basic decision rule would be to assign **μ** to the class c_i with the highest probability given the pattern **μ**, according to

$$P(c_i|\boldsymbol{\mu}) > \max\left\{P(c_j|\boldsymbol{\mu})\right\} \Rightarrow \boldsymbol{\mu} \in c_i \ , \ j = 1,\ 2,\ \ldots, C;\ j \neq i\,, \tag{3}$$

where $P(c_i|\boldsymbol{\mu})$ is the *a posteriori* probability, which can be expressed in terms of the *a priori* probability $P(c_i)$ of the class c_i, the probability $P(\boldsymbol{\mu})$ and the conditional probability $P(\boldsymbol{\mu}|c_i)$ as follows

$$P(c_i|\boldsymbol{\mu}) = \frac{P(\boldsymbol{\mu}|c_i)P(c_i)}{P(\boldsymbol{\mu})}\,. \tag{4}$$

Then, the decision rule of (3) can be rewritten as

$$P(\boldsymbol{\mu}|c_i)P(c_i) > \max\left\{P(\boldsymbol{\mu}|c_j)P(c_j)\right\} \Rightarrow \boldsymbol{\mu} \in c_i \ , \ j = 1,\ 2,\ \ldots, C;\ j \neq i\,. \tag{5}$$

In the moments space, the conditional probability $P(\boldsymbol{\mu}|c_i)$ could be established without difficulty since the moments follow a multivariate Gaussian law [24], with mean and covariance matrix estimated from the training stage. Usually, the classes are considered equiprobable, thus $P(c_j) = 1/C$.

k-nearest neighbors

The procedure to classify a pattern **μ** by the k-nearest neighbors (knn) technique involves the determination of the *k* training patterns closest to **μ** employing an appropriate distance metric. Therefore, **μ** is assigned to the class c_i, $i = 1, 2, \ldots, C$ with the largest number of representatives within the set of *k* nearest neighbors to **μ**. Among the variables to consider for the implementation of the method are the number of *k* neighbors, the distance metric and the training set to be used [25]. The most commonly used distance metrics in this classifier are the Euclidean, Minkowski, and Mahalanobis [11, 25]. The knn is not widely employed in modern radar. However, it is widely used as a benchmark to compare the performance of new algorithms [12, 26] or in combination with other classifiers [27].

Support Vector Machine

Classification using Support Vector Machine (SVM) for the basic case of two linearly separable classes takes as input a vector $\boldsymbol{\mu} \in \mathbb{R}^S$ and as output the set $y \in [1, -1]$. A training set with *B* pairs of the form $[(\boldsymbol{\mu}_1, y_1), (\boldsymbol{\mu}_2, y_2), \ldots, (\boldsymbol{\mu}_B, y_B)]$ is used during the supervised learning. The objective is to obtain the hyperplane that separates the pairs of different classes with the maximum margin. When the classes are linearly separable, a discriminant function $D(\boldsymbol{\mu})$ could be determined that satisfy [28]

$$D(\boldsymbol{\mu}) = \mathbf{h}^T\boldsymbol{\mu} + b\begin{cases} \geq 1 \rightarrow y = 1 \Rightarrow \boldsymbol{\mu} \in C_1 \\ < 1 \rightarrow y = -1 \Rightarrow \boldsymbol{\mu} \in C_2 \end{cases}, \tag{6}$$

TELEMÁTICA
REVISTA DIGITAL de las Tecnologías de la Información y las Telecomunicaciones
Revista Telemática. Vol. 4 No. 20 , Octubre-Diciembre, 2021, p.40- 51 ISSN 1729-3804

where **h** is an *S*-dimensional vector and *b* is a bias. When classes are not linearly separable, a transformation is employed that maps the training set into a higher-dimensional space, where linear separation is possible. The transformation is performed using linear, polynomial and Gaussian kernel functions [11, 25].

SVM-based classification has been widely applied to Synthetic Aperture Radar (SAR) images [29] and High-Resolution Range Profiles (HRRP) [15, 30, 31]. The authors of [31] compare the performance of several ATR methods, highlighting two SVMs with polynomial and Gaussian kernels. The results show that the performance of SVM is highly dependent on the target type and it is superior to the Bayesian and knn classifiers [31].

Artificial Neural Networks

Artificial Neural Networks (ANNs) consist of a large number of simple processors with multiple interconnections, where each processor models a neuron [32]. Neurons are organized into input, hidden and output layers. Figure 1 represents a diagram of an ANN with *I* layers and their basic elements [32]. For this work the input of the network is the pattern to be classified $\boldsymbol{\mu}$, which components are the *S* moments. The input of each layer together with the weight vector $\mathbf{w}^{(i)}$ are processed by a weight function. Then the result $\mathbf{W}^{(i)}$ and the bias $\mathbf{v}^{(i)}$ are subjected to the input function obtaining $\mathbf{V}^{(i)}$. Finally, the transfer or activation function is evaluated, resulting in the output layer vector $\mathbf{F}^{(i)}$. In the output layer, $\mathbf{F}^{(i)}$ will have as many components as classes to be classified.

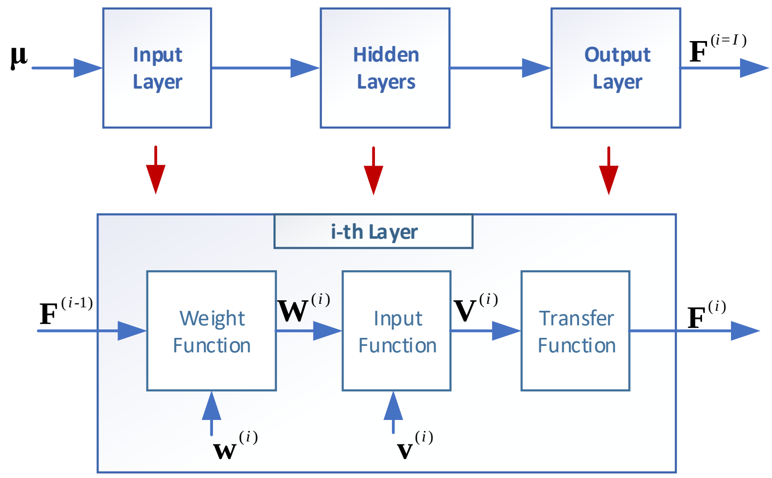

Figure 1: Simplified diagram of an ANN.

According to the topology, ANNs can be classified as feed-forward networks and recurrent or feed-backward networks [32, 33]. Feed-forward networks are characterized by the absence of feedback and the most common family within this category is the multilayer perceptron (MLP-NN). On the other hand, recurrent networks are distinguished by the presence of feedback connections. This results in a dynamic behavior that allows the network to consider previous inputs when making a decision regarding the current input [32]. In general, ANNs have been widely used for ATR employing various radar technologies. MLP-NNs and the feed-forward radial basis function neural networks (RBF-NNs) are very common [30, 34, 35].

4. EVALUATION OF SUPERVISED CLASSIFIERS USING THE MOMENTS SPACE

To evaluate the performance of the classifiers described in the previous section, three different coefficients are analyzed. The first one is the *accuracy* given by

$$A_{cc} = N_{cc} / \left(N_{cc} + N_e \right), \tag{7}$$

Where N_{cc} and N_e are the respective numbers of correctly and incorrectly classified patterns. Accuracy gives a measure of the overall performance of the classifier for all its classes [25].

The second coefficient is the *error rate*, defined as the ratio between the number of misclassified patterns to the total number of classifications, so it can be computed through

$$E_r = 1 - A_{cc}. \tag{8}$$

On the other hand, the third used coefficient is the *precision*, which evaluates the performance of the classifier for the class c_i according to

$$P_r = N_{c_i} \Big/ \left(N_{c_i} + N_{e_i} \right), \tag{9}$$

where N_{c_i} is the number of patterns of c_i properly classified and N_{e_i} corresponds to those erroneously classified.

For computation of the above coefficients, confusion matrices were obtained [25], which is another tool to evaluate the performance of a classifier [11, 25]. This square C x C matrix represents the output of the classifier in the evaluation stage and its (i, j) element indicates the number of patterns of class c_i assigned to class c_j. The larger the values of the matrix's diagonal, the better the performance of the classifier. Since we are only considering supervised learning, the algorithms adapt its parameters from the labeled data in order to discriminate the classes provided with the training set. To evaluate the performance, the unlabeled patterns from the evaluation set are used as input to the classifier and its response is compared with the previously known classes. To this end we split the database in a training and evaluation sets according to the k-fold cross-validation technique [25].

For the simulation of targets in the presence of marine clutter we use the Simulink model for an End-to-End Monostatic Radar, belonging to the Phased Array System Toolbox of Matlab R2016a [36]. The targets follow the Swerling III model [40] proposed in [7, 10, 37-39], which considers the existence of one main scatter and many minor scatters with slow fluctuations. For clutter simulation the results of [41, 42] were considered, so two Weibull models were taken for sea states with moderate waves of 1.27 m and smooth waves of 0.21 m (β = 4.79, α = 72.92 and β = 2.82, α = 33.29, respectively). Samples generated from these distributions were added to the targets.

To form the patterns, the first-order moment of first-order statistics ε_1, the second-order moment of first-order statistics ε_2 and the second-order moment of second-order statistics ε_3 were selected. The moment ε_1 have a direct relation to the RCS of targets [7, 37, 43-45], an important parameter for evaluating the scattering properties of objects. For the case of ε_2, in addition to including information regarding the RCS, it provides a measure of the signal variability or dispersion [16]. The greater the irregularity in terms of aspect angle and shape of the target, the greater the dispersion of the amplitude of the reflected wave and, therefore, the second-order moment. Finally, ε_3 provides a measure of the fluctuation degree of the echo-signal, since it is a monotonic function of the correlation coefficient [16].

The characteristics of the generated database are presented in Table 1, containing five targets for two sea states: smooth and moderate. The last two columns show two possible variants for the selection of classes: Variant A, which considers each class as a target/sea pair, resulting in a total of ten classes; and Variant B, which considers one class for each target, equivalent to five classes.

Table 1: Variants of classes considered.

Target	RCS [m^2]	Sea state	Variant A	Variant B
Target 1	1.5	Smooth	Class 1	Class 1
Target 1	1.5	Moderate	Class 2	Class 1
Target 2	5	Smooth	Class 3	Class 2
Target 2	5	Moderate	Class 4	Class 2
Target 3	10	Smooth	Class 5	Class 3
Target 3	10	Moderate	Class 6	Class 3
Target 4	20	Smooth	Class 7	Class 4
Target 4	20	Moderate	Class 8	Class 4
Target 5	30	Smooth	Class 9	Class 5
Target 5	30	Moderate	Class 10	Class 5

To select only one of the above variants a knn classifier with k = 1 is used and the confusion matrices of Figure 2 are obtained. It can be seen in part (a) that the classifier performs very poorly with an error rate of 0.4522, so it generates

Revista Telemática. Vol. 4 No. 20 , Octubre-Diciembre, 2021, p.40- 51 ISSN 1729-3804

an incorrect output 45.22% of the time. Note that most of these misclassifications occur between classes representing the same target with different sea state. This drawback does not occur for the second variant of Figure 2 (b), where the error rate is 5.6 %, which is adequate for practical purposes.

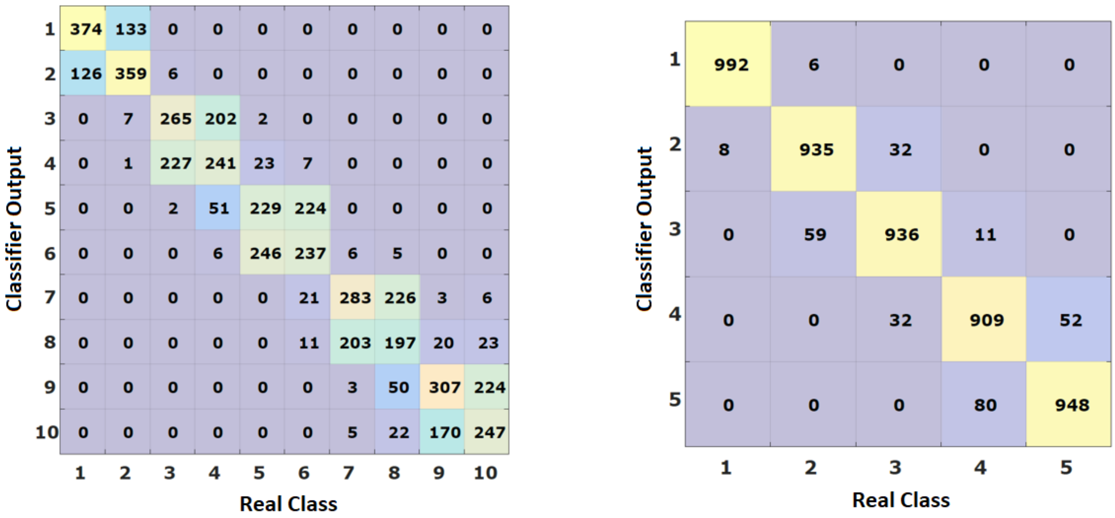

(a) (b)

Figure 2: Confusion matrix considering ten (a) and five (b) classes for the variants of Table 1.

The performance when changing the sea state was also analyzed. For this purpose, the 1nn classifier is trained in smooth sea and evaluated when this state is maintained, obtaining an error rate of 1.36 %. On the other hand, the result is 16.56 % when the classifier is trained in smooth sea and operates over moderate sea. These results suggest the need to train the classifier with samples obtained in both states. Since this work don’t pursue the recognition of different sea states, the variant B of Table 1 will be used for the remaining experiments.

Bayesian classifier

The accuracy of the Bayesian classifier is computed for the sets of moments and random-sample sizes (M) listed in Table 2. The highest accuracy of 91.66 % is achieved when three moments are used and M = 128, while the accuracy decreases to 85.3 % when M = 64. Figure 3 shows the confusion matrices for the three moments set.

Table 2: Accuracy of the Bayesian classifier for different sets of moments and random-sample size.

Set of moments	ε_1	ε_2	ε_3	ε_1, ε_3	ε_1, ε_2, ε_3
Accuracy [%] for M = 128	77.22	75.06	85.26	87.56	91.66
Accuracy [%] for M = 64	69.65	68.87	77.34	80.71	85.3

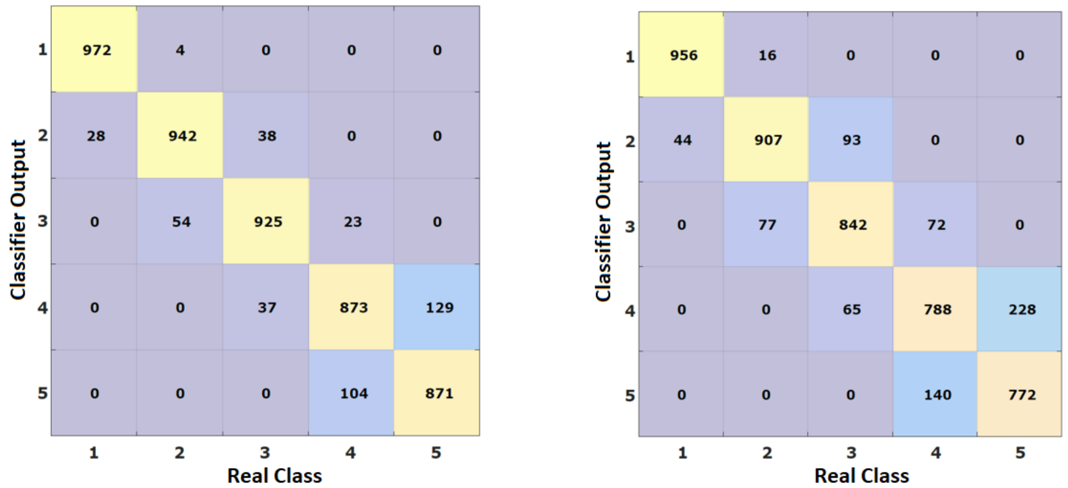

(a) (b)

Figure 3: Confusion matrices for the Bayesian classifier using ε_1, ε_2 and ε_3 with M = 128 (a) and M = 64 (b).

K - Nearest Neighbors

As part of the knn, three different classifiers were implemented according to the above-mentioned distance metrics. The main design variable of this classifier is the number of k neighbors to be used. Table 3 shows the accuracy of the classifier with Euclidean distance when k varies, reaching its highest value for k = 3.

Table 3: Accuracy of the knn classifier with Euclidean distance for various values of k.

k	1	3	5	7
Accuracy [%]	94.56	94.64	94.02	93.54

It is interesting to analyze how much the results of the knn classifier vary when changing the distance metric. For this purpose, Euclidean, Minkowski (with exponent equal to 3 [25]) and Mahalanobis distances [11] were considered. The performance of the knn classifier with k = 3, employing the Minkowski distance (A_{cc} = 94.68%) does not differ much from that using the Euclidean metric (A_{cc} = 94.64%). On the other hand, when using the Mahalanobis distance the classifier reaches 97.8% accuracy, with the disadvantage of requiring more processing time than the previous ones, mainly due to the need of estimating the covariance matrix. The confusion matrices for each case are shown in Figure 4.

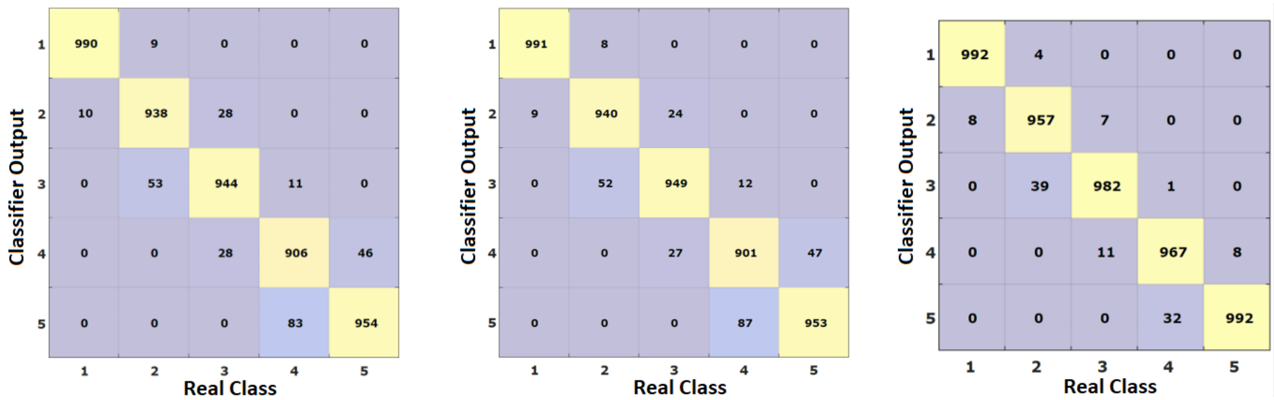

(a) (b) (c)

Figure 4: Confusion matrix for knn classifier with k =3 for Euclidian (a), Minkowski (b) and Mahalanobis (c) distances.

Support Vector Machines

Two SVM classifiers were implemented, one radial-basis function with Gaussian kernel (RBF-SVM) and the other with polynomial kernel (PK-SVM). As shown in Table 4, for the polynomial kernel the 1st, 2nd and 3rd degrees were considered, obtaining the best result for the 2nd degree. For the RBF-SVM classifier, scaling factors 0.43, 1.7 and 6.9

TELEMÁTICA
REVISTA DIGITAL de las Tecnologías de la Información y las Telecomunicaciones
Revista Telemática. Vol. 4 No. 20 , Octubre-Diciembre, 2021, p.40- 51 ISSN 1729-3804

were used, obtaining the best performance in the first case. Figure 5 shows the confusion matrices for the RBF-SVM classifiers with scale factor 0.43 and PK-SVM of 2nd degree.

Table 4: Accuracy of RBF-SVM and PK-SVM classifiers.

RBF-SVM	Scaling Factors	Accuracy [%]
	0.43	93.4
	1.7	91.56
	6.9	84.74
PK-SVM	Degrees	Accuracy [%]
	1st	63
	2nd	91.9
	3rd	62.22

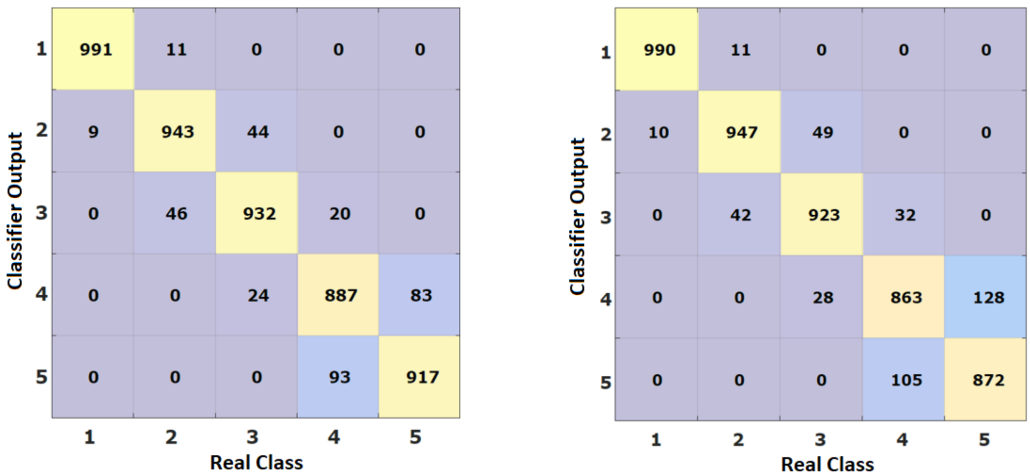

(a) (b)

Figure 5: Confusion matrix for RBF-SVM with scale factor 0.43 (a) and PK-SVM of 2nd degree (b).

Artificial Neural Networks

Two types of ANNs were implemented: RBF-NN and MLP-NN, using in both cases the Matlab Neural Network Toolbox [33]. Both have two layers, where the output layer has five neurons, since this is required to distinguish five classes. The weight vectors are obtained during the training stage of the network, using the scaled conjugate gradient backpropagation method [32, 33] and the networks details are described in previous works [32, 33, 46].

In the RBF-NN the first layer has many neurons as elements in the training set. The bias of this layer is computed from the dispersion coefficient at the output [33, 46]. The performance of the RBF-NN was evaluated considering the dispersion values of 0.01, 0.1 and 1, obtaining accuracies of 77 %, 77.02% and 55.74 %, respectively. The confusion matrix for the dispersion of 0.1 is shown in part (a) of Figure 6. RBF-NN networks employ a larger number of neurons than MLP-NN networks, but generally require less training time.

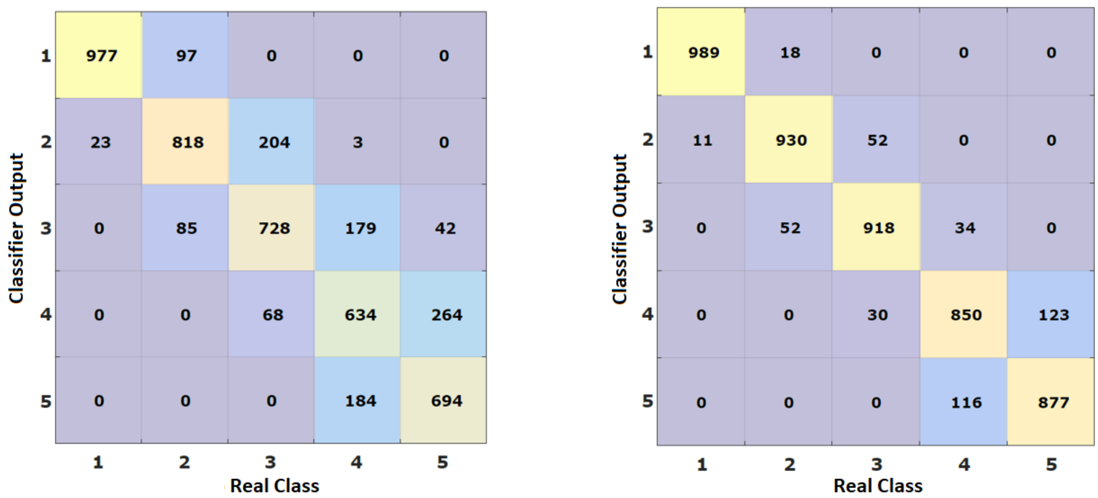

(a) (b)

Figure 6: Confusion matrix for the RBF-NN classifier with dispersion 0.1 (a) and for MLP-NN (b).

In the case of the MLP-NN, both input and output layers were designed considering the scalar product weight function and the input function as a sum function. Both layers use biases obtained during the training stage using the scaled conjugate gradient backpropagation method [32, 33]. The MLP-NN network allows a number of parameters to be defined, including the number of neurons in the hidden layer and the activation function for both layers. To define the number of neurons, the accuracy of an MLP-NN with hyperbolic tangent and Softmax activation functions [25] for the hidden and output layers, respectively, was tested for 4 to 20 neurons in the hidden layer. All results were in an accuracy range between 91.2% and 91.28% so it was decided to use 10 neurons.

To select the activation function for the hidden layer, the following variants were considered: logistic sigmoid, hyperbolic tangent, and Elliot sigmoid [25, 32]. While for the output layer the Linear, Competitive and Softmax functions [25, 32] were used. When Softmax is used as the activation function for the output layer, the network performs better than in the remaining cases, where 50% accuracy was not achieved. The best results were obtained for the combinations listed in Table 5. The confusion matrix for the best case is shown in part (b) of Figure 6. It was found that the variation of the activation function of the hidden layer does not have much influence on the performance of the MLP-NN classifier, at least for the three functions used.

Table 5: Accuracy of the MLP-NN classifier for various activation functions.

Hidden Layer	Output Layer	Accuracy [%]
Hyperbolic tangent	Softmax	91.28
Elliot sigmoid	Softmax	91.04
Logistic sigmoid	softmax	90.66

5. CONCLUSIONS

Table 6 shows a summary of the best-performing supervised classifiers previously considered. The classifiers with the highest accuracy are knn (k = 3) with Mahalanobis distance and RBF-SVM with scale factor 0.43. The knn with Mahalanobis distance provides a superior accuracy (97.8 %), but requires more classification time than the RBF-SVM. To analyze the storage consumption, it is necessary to recall that knn uses the distance between the pattern and its nearest neighbors, so it requires the storage of the labeled patterns. On the other hand, RBF-SVM computes the separation hyperplanes between classes through training and only needs to store its coefficients. The classification time and computational resources requirements vary depending on the final implementation platform.

Table 6: Accuracy and precision of the best-performing classification algorithms analyzed.

		Precision [%]				
Classification method	Accuracy [%]	Class 1	Class 2	Class 3	Class 4	Class 5
Bayesian classifier	91.66	99.59	93.45	92.32	84.02	89.33
knn (k = 3, Mahalanobis distance)	97.80	99.60	98.46	96.09	98.07	96.88
RBF-SVM (scale 0,43)	93.40	98.90	94.68	93.39	89.24	90.79

Revista Telemática. Vol. 4 No. 20 , Octubre-Diciembre, 2021, p.40- 51 ISSN 1729-3804

MLP-NN	91.28	98.21	93.66	91.43	84.75	88.32

Using the moments space as input features, it is possible to effectively classify various types of radar targets. This is revealed through the high accuracy (greater than 91%) and precision (greater than 84%) values of the main supervised classification methods reported in the literature. On the other hand, the moments computation only involves accumulation and multiplication operations, which does not require high complexity of hardware/software resources.

REFERENCES

[1] B. Snapir, T. W. Waine, and L. Biermann, "Maritime vessel classification to monitor fisheries with sar: Demonstration in the North Sea," Remote Sensing, vol. 11, no. 3, p. 353, 2019.
[2] S. Ünlü, B. Alpar, and B. Öztürk, Oil Spill Along the Turkish Straits Sea Area: Accidents, Environmental Pollution, Socio-Economic Impacts and Protection. Turkish Marine Research Foundation, 2018, p. 480.
[3] P. Huang, Q. Shi, W. Xu, and W. Tan, "Research on Yellow River Ice Supervised Classification Method Based on Polarimetric SAR Data," 2019 IEEE International Conference on Signal, Information and Data Processing (ICSIDP), pp. 1-5, 2019.
[4] Z.-X. Guo and P.-L. Shui, "Anomaly-based Sea-surface Small Target Detection using K-Nearest Neighbour Classification," IEEE Transactions on Aerospace and Electronic Systems, 2020.
[5] M. Leclerc, R. Tharmarasa, M. C. Florea, A.-C. Boury-Brisset, T. Kirubarajan, and N. Duclos-Hindié, "Ship classification using deep learning techniques for maritime target tracking," in 2018 21st International Conference on Information Fusion (FUSION), 2018, pp. 737-744: IEEE.
[6] F. Yang, J. Le Kernec, F. Fioranelli, and Q. Liu, "Shape feature aided target detection method for micro-drone surveillance radar," IET International Radar Conference (IET IRC 2020), 2020.
[7] M. A. Richards, Fundamentals of Radar Signal Processing, Second ed. McGraw-Hill Education, 2014.
[8] J. S. Patel, F. Fioranelli, and D. Anderson, "Review of radar classification and RCS characterisation techniques for small UAVs ordrones," IET Radar, Sonar & Navigation, vol. 12, no. 9, pp. 911-919, 2018.
[9] Seung-Jae Lee et al., "Classification of Shell-Shaped Targets Using RCS," IEEE Transactions on Antennas and Propagation, vol. 64, no. 4, 2016.
[10] J. R. S. Gálvez, N. C. Ferry, and M. V. Pozo, "Campo dispersado por pequeños blancos de radar situados sobre la superficie del mar," Ingeniería Electrónica, Automática y Comunicaciones, vol. 41, no. 1, pp. 89-100, 2020.
[11] S. Theodoridis and K. Koutroumbas, Pattern Recognition 4th ed. Elsevier, 2009.
[12] J. Liu, N. Fang, Y. J. Xie, and B. F. Wang, "Radar target classification using support vector machine and subspace methods," IET Radar, Sonar and Navigation, vol. 9, no. 6, pp. 632-640, 2015.
[13] J. A. Garzon-Guerrero, D. P. Ruiz, and M. C. Carrion, "Classification of geometrical targets using natural resonances and principal components analysis," IEEE transactions on antennas and propagation, vol. 61, no. 9, pp. 4881-4884, 2013.
[14] J. Liu, N. Fang, Y. J. Xie, and B. F. Wang, "Multi-scale feature-based fuzzy-support vector machine classification using radar range profiles," IET Radar, Sonar & Navigation, vol. 10, no. 2, pp. 370-378, 2016.
[15] L. Wenbo, Y. Jiawen, Z. Gong, and S. Qian, "HRRP target recognition based on kernel joint discriminant analysis," Journal of Systems Engineering and Electronics, vol. 30, no. 4, pp. 703-708, 2019.
[16] C. Guillén, N. Chávez, and J. Bacallao, "Radar detection in the moments space with constant false alarm rate," Digital Signal Processing, 2021.
[17] N. Chávez and C. Guillén, "Radar detection in the moments space of the scattered signal parameters," Digital Signal Processing vol. 83 pp. 359–366, 2018.
[18] C. Guillén and N. Chávez, "Decision Rules for Radar Detection in the Moments Space with Arbitrary Correlation Degree and Constant False Alarm Rate," presented at the IWAIPR 2021, 2021. Available: https://doi.org/10.1007/978-3-030-89691-1_40
[19] C. Guillén, G. Casas, D. Frómeta, and N. Chávez, "Simple Communication Interface for a Radar Detector in the Moments Space," International Journal of Engineering and Technology Innovation, vol. 9, no. 4, pp. 314-326, 2019.
[20] A. Papoulis, Probability, Random Variables, and Stochastic Processes, 3rd ed. McGraw-Hill, 1991.
[21] P. Z. Peebles, Probability, Random Variables and Random Signals Principles, 2nd ed. MacGraw-Hill, 1987.
[22] M. Meller, "On Bayesian Tracking and Prediction of Radar Cross Section," IEEE Transactions on Aerospace and Electronic Systems, vol. Early Access Article, 2018.

[23] A. C. Turlapaty, "Shape parameter estimation for K-distribution using variational bayesian approach," presented at the IEEE Workshop on Statistical Signal Processing, Freiburg, Germany, 2019.
[24] C. Guillén, G. Rodríguez, and N. Chávez, "Selection of Sampling Interval and Size of Random Sample for Radar Detection in the Moments Space," Periodica Polytechnica Electrical Engineering and Computer Science, vol 65, no. 4, 2021.
[25] Andrew R. Webb and K. D. Copsey, Statistical Pattern Recognition, Third ed. United Kingdom: John Wiley & Sons, 2011.
[26] C. Carmona-Duarte, M. Á. Ferrer-Ballester, J. Calvo-Gallego, and B. P. Dorta-Naranjo, "Vessel Identification Study for Non-Coherent HighResolution Radar," presented at the 2013 47th International Carnahan Conference on Security Technology (ICCST), 2013.
[27] C. M. Pilcher and A. Khotanzad, "Maritime ATR using Classifier Combination and High Resolution Range Profiles," IEEE Transactions on Aerospace and Electronic Systems, vol. 47, no. 4, pp. 2558-2573, 2011.
[28] A. Shigeo, Support Vector Machines for Pattern Classification, 2nd ed. (Advances in Pattern Recognition). Springer, 2010.
[29] P. L. Cross, "Maritime automated targets recognition algorithm test bed for high resolution ISAR imagery," in 2013 IEEE International Conference on Technologies for Homeland Security (HST), 2013, pp. 369-374.
[30] M. J. Sagayaraj, V. Jithesh, and D. Roshani, "Comparative Study Between Deep Learning Techniques and Random Forest Approach for HRRP Based Radar Target Classification," International Conference on Artificial Intelligence and Smart Systems (ICAIS), pp. 385-388, 2021.
[31] T. Jasinski, I. Antipov, S. T. Monteiro, and G. Brooker, "W-Band Maritime Target Classification using High Resolution Range Profiles," presented at the International Conference on Radar 2013, Adelaide, SA, Australia, 2013.
[32] C. C. Aggarwal, Neural Networks and Deep Learning, Primera ed. (A Textbook). Springer, 2018.
[33] MathWork. (2018). Neural Network Toolbox Documentation. Available: https://www.mathworks.com/products/neural-network.html
[34] A. Jakubiak, "Classification of Weather Clutter Models using Neurals Networks," TCSET, 2004.
[35] C. Zhao, X. He, J. Liang, T. Wang, and C. Huang, "Radar HRRP Target Recognition via Semi-Supervised Multi-Task Deep Network," IEEE Access, vol. 7, pp. 114788-114794, 2019.
[36] MathWorks, "Phased Array System Toolbox," 2018.
[37] M. I. Skolnik, Introduction to Radar Systems, Third ed. McGraw-Hill Education, 2001.
[38] D. O. González and Y. G. Morales, "Cálculo de la permitividad dieléctrica compleja de los materiales absorbentes dieléctricos con pérdidas," [Tesis presentada en opción al título de Ingeniero en Telecomunicaciones y Electrónica], Departamento de Telecomunicaciones y Telemática, Universidad Tecnológica de La Habana "José Antonio Echeverría" CUJAE, La Habana, 2016.
[39] H. M. Sathyendra and B. D. Stephan, "Effects of Using Enhanced Input Range Profiles for 1-d Automated Maritime Vessel Classification," presented at the 2014 IEEE Radar Conference, Cincinnati, OH, USA, 2014.
[40] C. Guillén and N. Chávez, "Algorithms to Generate Random Samples following the Swerling Models," Revista Cubana de Ciencias Informáticas, vol. 13, no. 2, pp. 1-12, 2019.
[41] Seishiro Ishii, Syuji Sayama, and K. Mizutani, "Effect of Changes in Sea-Surface State on Statistical Characteristics of Sea Clutter with X-band Radar " Wireless Engineering and Technology, no. 2, pp. 175-183, 2011.
[42] J. R. Machado Fernández and J. d. l. C. Bacallao Vidal, "Distribuciones estadísticas para modelar clutter marino: una revisión," RIELAC- Revista de Ingeniería Electrónica, Automática y Comunicaciones, vol. XXXVIII no. 2, pp. 12-35 Mayo – Agosto 2017.
[43] K. Ward, R. Tough, and S. Watts, Sea Clutter Scattering, the K Distribution and Radar Performance, 2nd ed. London, U. K: The Institution of Engineering and Technology, 2013.
[44] M. A. Richards, J. A. Scheer, and W. A. Holm, Principles of Modern Radar Vol. I: Basic Principles. Raleigh, NC, USA: SciTech Publishing, 2010.
[45] M. I. Skolnik, Radar Handbook, 3ra ed. MacGraw-Hill, 2008.
[46] L. M. Marrero, "Propuesta de un Algoritmo Efectivo para la Clasificación Automática de Blancos en Presencia de Clutter Marino Empleando un Radar Naval," [Tesis presentada en opción al título de Master en Telecomunicaciones y Electrónica], Departamento de Telecomunicaciones y Telemática, Universidad Tecnológica de La Habana "José Antonio Echeverría" CUJAE, La Habana, 2018.

AUTHOR SECTION

Yusleidy Alvarez Germade received the B.S. in Telecommunications and Electronics (2010) from the Technological University of Havana José Antonio Echeverría, CUJAE. She currently serves as Instructor Professor and researcher with the Departament of Telecommunications and Telematics of the previous institution. Her research interests include digital signal processing and pattern recognition.

Revista Telemática. Vol. 4 No. 20 , Octubre-Diciembre, 2021, p.40- 51 ISSN 1729-3804

Camilo Guillén Soriano received the B.S. in Telecommunications and Electronics (2013), the M.S. in Digital Systems (2018) and the Ph.D. (2021) from the Technological University of Havana José Antonio Echeverría, CUJAE. He currently serves as Auxiliar Professor and researcher with the Departament of Telecommunications and Telematics of the previous institution. His research interests include digital signal processing and pattern recognition. Member of the Cuban Association of Pattern Recognition (ACRP) since 2015.

Liz Martínez Marrero received the B.S. in Telecommunications and Electronics (2012) and M.S. in Telecomunications (2018) from the Technological University of Havana José Antonio Echeverría, CUJAE. She is currently working toward the Ph.D. degree as a Doctoral Researcher at the Interdisciplinary Centre for Security, Reliability, and Trust (SnT) of the University of Luxembourg. Her research interests include digital signal processing for wireless communications, focusing on the physical layer, satellite communications, and carrier synchronization for distributed systems.

Nelson Chávez Ferry received the B.S in Electrical Engineer, specialty in Telecommunications (1966), from the Faculty of Technology of the University of Havana; the degree of Candidate in Technical Sciences (1978) from the Naval Academy of the Soviet Union, recognized in Cuba as Doctor in Technical Sciences and the degree of Doctor of Science (2002). Currently is a Full and Consultant professor with the Departament of Telecommunications and Telematics of the Technological University of Havana José Antonio Echeverría, CUJAE. He is the scientific leader of the Radar Group of this department and his research interests include radar target detection and recognition. Member of the Cuban Association of Pattern Recognition (ACRP) since 2015.

CONFLICT OF INTEREST

The authors declare no conflict of interests.